

Strain-enhanced photoluminescence from Ge direct transition

T.-H. Cheng,¹ K.-L. Peng,² C.-Y. Ko,² C.-Y. Chen,² H.-S. Lan,² Y.-R. Wu,¹ C. W. Liu,^{1,2,3,a)} and H.-H. Tseng⁴

¹Graduate Institute of Photonics and Optoelectronics and Department of Electrical Engineering, National Taiwan University, Taipei 10617, Taiwan

²Graduate Institute of Electronics Engineering and Department of Electrical Engineering, National Taiwan University, Taipei 10617, Taiwan

³National Nano Device Laboratory, Hsinchu 30078, Taiwan

⁴Ingram School of Engineering, Texas State University, San Marcos, Texas 78666, USA

(Received 19 March 2010; accepted 21 April 2010; published online 24 May 2010)

Strong enhancement of Ge direct transition by biaxial-tensile strain was observed. The reduction in band gap difference between the direct and indirect valleys by biaxial tensile strain increases the electron population in the direct valley, and enhances the direct transition. The band gap reduction in the direct and indirect valleys can be extracted from the photoluminescence spectra and is consistent with the calculations using $k \cdot p$ and deformation potential methods for conduction bands and valence bands, respectively. © 2010 American Institute of Physics. [doi:10.1063/1.3429085]

One of the most attractive areas of research in group IV semiconductors is seeking the possibility of optoelectronic applications using indirect band gap materials.^{1–4} Germanium is expected to be the possible candidate due to its high carrier mobility, strong photon absorption, and Si compatibility. Recently, many methods are reported to enhance direct radiative transition from Ge, including the high doping concentration, the elevated temperature, high pumping power, and epitaxial strain^{5–9} originated from thermal expansion. However, the reported strain was originated from the misfit of thermal expansion coefficients between the epitaxial Ge layer and the Si substrate during the cooling process and the control of such epitaxial strain was not technologically convenient. In this work, mechanical strain is applied to enhance direct transition as compared to indirect transition from Ge, and both the direct and indirect band gap reductions by strain can be extracted from the photoluminescence (PL) spectra.

The n-type Sb-doped Ge (100) substrate was used in this study. The pumping laser of PL has the wavelength of 671 nm and the power of 360 mW. The InGaAs detector has the detection window from 1.4 to 2.1 μm to cover the emissions for both direct and indirect transitions. Note that the absorption length of Ge at the wavelength of 671 nm is ~ 110 nm. The experimental setup for PL measurement and the mechanism to apply external mechanical strain were reported previously in Ref. 10. The Raman spectroscopy was used to determine the amount of strain applied on Ge.

The PL spectra of the bulk (100) Ge with different resistivity shows different characteristics at 0.78 eV for the direct transition (Fig. 1). The Ge with low resistivity (0.005–0.02 $\Omega\text{ cm}$) shows more significant direct band transition as compared to the Ge with high resistivity (1–10 $\Omega\text{ cm}$). For bulk Ge and Ge-on-insulator, the PL intensity of direct transition increases with the donor concentration was reported in Ref. 11. The electrons were pumped from valence bands to the conduction band near the Γ valley, and then, relaxed to the conduction band edge at the Γ valley as well as at L valleys by scattering.⁵ The electrons in the

direct (Γ) and indirect (L) valleys recombine with holes in the valence bands and emit the infrared with the energy around 0.78 eV and 0.7 eV, respectively (Fig. 1). The Ge with higher electron concentration moves the electron Fermi energy closer to the conduction band edge under the same pumping power. Due to the Fermi–Dirac distribution, the upshift in electron Fermi level increases the relative electron concentration at the Γ valley with respect to L valleys. Therefore, low-resistivity Ge has stronger direct transition than high-resistivity Ge.¹¹

Under the laser excitation, most of the electrons are pumped into the indirect valleys with lower energy following the Fermi distribution. In order to have a sufficient number of electrons in the direct valley of the conduction band, the external biaxial tensile strain is introduced. The band structure of relaxed Ge and biaxial tensile strained Ge are schematically shown in Fig. 2. The relaxed Ge has a 660 meV indirect band gap at the L valleys and a 800 meV direct band gap at the Γ valley at room temperature.⁷ The indirect band gap of Ge is smaller than the direct gap by only 140 meV [Fig. 2(a)]. By applying biaxial tensile strain, the conduction band in Γ valley moves downward with respect to the vacuum level, and the valence band splits into heavy hole

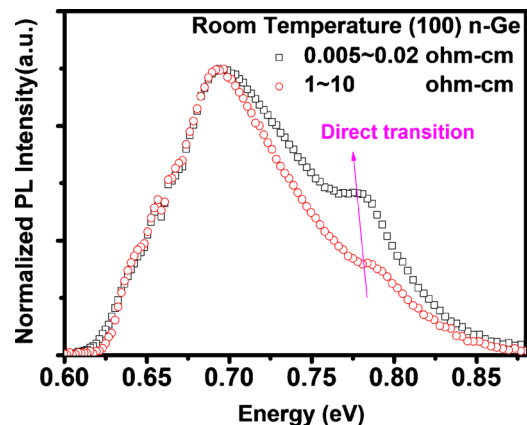


FIG. 1. (Color online) The PL spectra of the n-type bulk Ge (100) with different resistivity. The direct transition from the Γ valley is more significant in Ge with lower resistivity.

^{a)}Author to whom correspondence should be addressed. Electronic mail: chee@cc.ee.ntu.edu.tw.

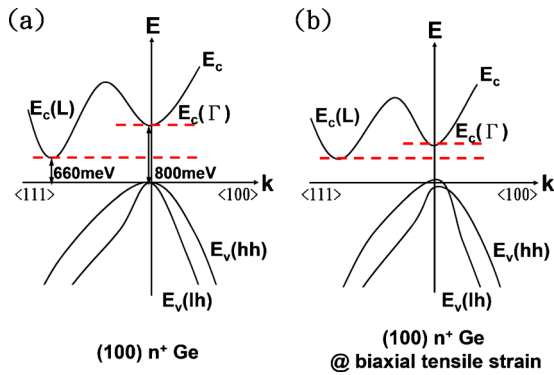


FIG. 2. (Color online) (a) The band structure of n-type Ge and (b) the schematic diagrams of the band gap reduction in L and Γ valleys with biaxial tensile strain. More electrons populate in the Γ valley due to the reduction in the difference between direct and indirect band gaps.

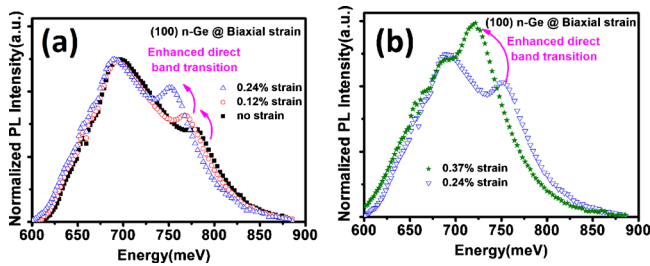


FIG. 3. (Color online) PL spectra of n-type bulk Ge (100) under biaxial tensile strain at room temperature. The intensity of direct band gap transition increases with increasing strain.

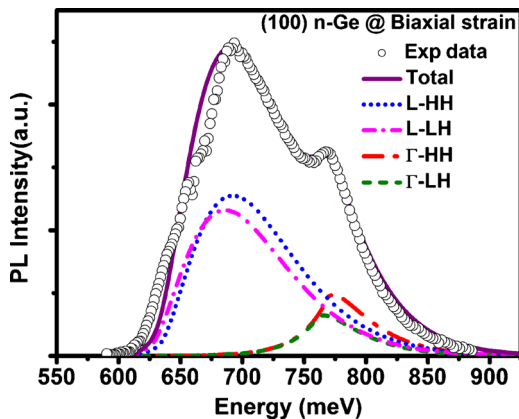


FIG. 4. (Color online) The PL spectrum of strained-Ge (0.12%) fitted by the direct transition and indirect transition models. The transitions from conduction band of direct and indirect valleys to HH and LH bands contribute to the strained-Ge optical transitions.

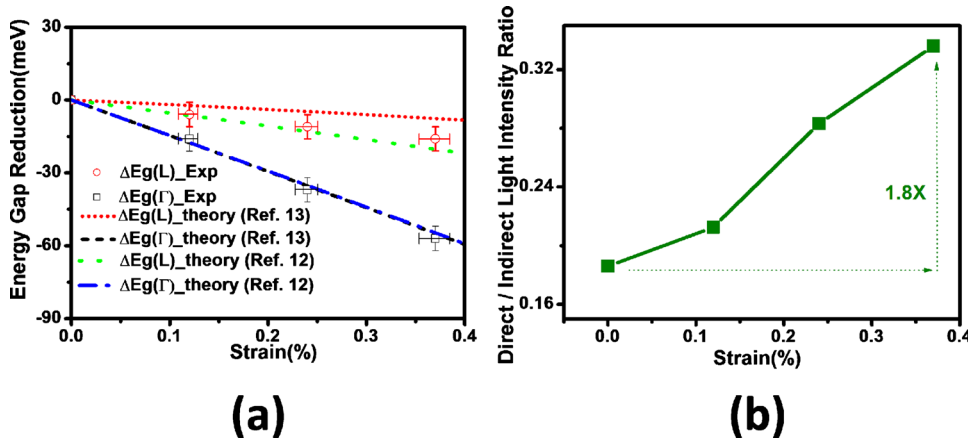


FIG. 5. (Color online) (a) The strain induced band gap reduction in both direct and indirect valleys with biaxial tensile strain. (b) The radiative recombination intensity ratio of direct to indirect transitions. The direct-to-indirect intensity ratio is enhanced by 1.8 times under 0.37% strain.

(HH) and light hole (LH) bands⁶ [Fig. 2(b)]. Depending on the parameters used in the deformation potential calculation, Ref. 12 shows the L valleys move downwards in energy, while Ref. 13 shows the opposite trend. The tensile strain shrinks the direct band gap more than the indirect band gap¹² and increases the electron population in the direct valley under the same pumping power.

Figures 3(a) and 3(b) show the PL enhancement of the direct band gap transition from n-type bulk Ge (100) with biaxial tensile strain at room temperature. The direct band gap transition becomes more and more significant by increasing the biaxial tensile strain up to 0.37%. Further strain broke the Ge sample in our mechanical setup. The redshift in the PL spectra under mechanical tensile strain reflects the band gap shrinkage, similar to the results of metal-oxide-semiconductor light-emitting diodes.¹⁴ There are two factors to enhance the direct band gap transition by applying biaxial tensile strain. First, more electrons transfer from L valleys to Γ valley due to the reduction in band gap difference between the direct band and the indirect bands. Second, the band gap reduction due to tensile strain enhances the absorption⁷ of the injected photons, and increases electron carrier density which shifts the electron Fermi level upwards.

In Fig. 4, the PL spectrum of the Ge under 0.12% biaxial tensile strain can be fitted by theoretical models. Both the electron-hole plasma recombination model¹⁴ and the direct band gap recombination model¹¹ are used to fit the experimental data. The introduction of a high concentration of doping or impurity will cause a perturbation of the band structure.⁶ The parabolic distribution of the states will be disturbed and prolonged by a tail extending into the energy gap. Due to the tail in the band gap, the experimental PL from Ge direct transition extends a little more into longer wavelengths compared to what was predicted by band-to-band transition model. Therefore, the band tail of exponential absorption edge¹⁵ was interpreted as reflecting tails of states into the energy gap. It is also taken into account in the direct band gap recombination model. Because the strain-induced splits at the valence bands, the PL spectra has the combination of multitransitions—L valleys to LH band, L valleys to HH band, Γ valley to LH band, and Γ valley to HH band.

Figure 5(a) shows the band gap reduction in theoretical calculation and the extracted data. The deformation potential and 6×6 $k \cdot p$ methods are used to calculate the conduction band and the valence band, respectively.^{16,17} Theoretical calculation shows the band gap reduction of 55 meV for direct transition at the strain of 0.37% using the calculation param-

eters in Refs. 12, 13, and 18. The band gap reduction in indirect transition is also shown in Fig. 5(a) using the parameters in Refs. 12 and 13. The experimental error bars are determined by the line width of Raman spectra and the fitting variation in our transition models. Figure 5(b) shows the intensity ratio of direct to indirect transition as a function of biaxial strain. Due to the reduction in the band gap difference between direct and indirect valleys, the intensity ratio of direct to indirect transition is enhanced by ~ 1.8 times at 0.37% biaxial tensile strain.

The strain can be an extra factor to enhance the direct transition of Ge. From our PL data, the enhancement can be up to ~ 1.8 times with 0.37% strain. Theoretically, Ge can become direct gap material at $\sim 2\%$ tensile strain according to the deformation potential calculation.¹² The progressive improvement of the radiative recombination makes it possible to have Ge-based light emitting devices and chip-to-chip optical interconnect for practical applications.

This work is supported by National Science Council of ROC under Contract Nos. 97-2221-E-002-229-MY3 and 98-2120-M-002-007-.

¹M. A. Green, J. Zhao, A. Wang, P. J. Reece, and M. Gal, *Nature (London)* **412**, 805 (2001).

²C. W. Liu, M. H. Lee, M.-J. Chen, I. C. Chen, and C.-F. Lin, *Appl. Phys. Lett.* **76**, 1516 (2000).

- ³H. Presting, T. Zinke, A. Splett, H. Kibbel, and M. Jaros, *Appl. Phys. Lett.* **69**, 2376 (1996).
- ⁴J. C. Sturm, H. Manoharan, L. C. Lenchyshyn, M. L. Thewalt, N. L. Rowell, J.-P. Noël, and D. C. Houghton, *Phys. Rev. Lett.* **66**, 1362 (1991).
- ⁵C. Li, Y. Chen, Z. Zhou, H. Lai, and S. Chen, *Appl. Phys. Lett.* **95**, 251102 (2009).
- ⁶X. Sun, J. Liu, L. C. Kimerling, and J. Michel, *Appl. Phys. Lett.* **95**, 011911 (2009).
- ⁷J. Liu, X. Sun, D. Pan, X. Wang, L. C. Kimerling, T. L. Koch, and J. Michel, *Opt. Express* **15**, 11272 (2007).
- ⁸S.-L. Cheng, J. Lu, G. Shambat, H.-Y. Yu, K. Saraswat, J. Vuckovic, and Y. Nishi, *Opt. Express* **17**, 10019 (2009).
- ⁹T.-H. Cheng, C.-Y. Ko, C.-Y. Chen, K.-L. Peng, G.-L. Luo, C. W. Liu, and H.-H. Tseng, *Appl. Phys. Lett.* **96**, 091105 (2010).
- ¹⁰M. H. Liao, M.-J. Chen, T. C. Chen, P.-L. Wang, and C. W. Liu, *Appl. Phys. Lett.* **86**, 223502 (2005).
- ¹¹M. El Kurdi, T. Kociniowski, T.-P. Ngo, J. Boulmer, D. Débarre, P. Boucaud, J. F. Damlencourt, O. Kermerrec, and D. Bensahel, *Appl. Phys. Lett.* **94**, 191107 (2009).
- ¹²C. G. Van de Walle, *Phys. Rev. B* **39**, 1871 (1989).
- ¹³M. V. Fischetti and S. E. Laux, *J. Appl. Phys.* **80**, 2234 (1996).
- ¹⁴M. H. Liao, T.-H. Cheng, and C. W. Liu, *Appl. Phys. Lett.* **89**, 261913 (2006).
- ¹⁵J. I. Pankove, *Phys. Rev.* **140**, A2059 (1965).
- ¹⁶P. H. Lim, S. Park, Y. Ishikawa, and K. Wada, *Opt. Express* **17**, 16358 (2009).
- ¹⁷C. Y.-P. Chao and S. L. Chuang, *Phys. Rev. B* **46**, 4110 (1992).
- ¹⁸J. Liu, D. D. Cannon, K. Wada, Y. Ishikawa, D. T. Danielson, S. Jongthammanurak, J. Michel, and L. C. Kimerling, *Phys. Rev. B* **70**, 155309 (2004).